




First Constraining Upper Limits on Gravitational-wave Emission from NS 1987A in SNR 1987A

Benjamin J. Owen¹ , Lee Lindblom², and Luciano Soares Pinheiro¹¹ Department of Physics and Astronomy, Texas Tech University, Lubbock, TX 79409-1051, USA² Center for Astrophysics and Space Sciences, University of California at San Diego, La Jolla, CA 92093-0424, USA

Received 2022 June 2; revised 2022 July 26; accepted 2022 July 28; published 2022 August 11

Abstract

We report on a search for continuous gravitational waves (GWs) from NS 1987A, the neutron star born in SN 1987A. The search covered a frequency band of 75–275 Hz, included a wide range of spin-down parameters for the first time, and coherently integrated 12.8 days of LIGO data below 125 Hz and 8.7 days of LIGO data above 125 Hz from the second Advanced LIGO–Virgo observing run. We found no astrophysical signal. We set upper limits on GW emission as tight as an intrinsic strain of 2×10^{-25} at 90% confidence. The large spin-down parameter space makes this search the first astrophysically consistent one for continuous GWs from NS 1987A. Our upper limits are the first consistent ones to beat an analog of the spin-down limit based on the age of the neutron star and hence are the first GW observations to put new constraints on NS 1987A.

Unified Astronomy Thesaurus concepts: Gravitational waves (678); Neutron stars (1108); Supernova remnants (1667)

Supporting material: data behind figure

1. Introduction

Due to the detection of neutrinos from the supernova (Bionta et al. 1987; Hirata et al. 1987), it has been known since 1987 that SN 1987A probably produced a neutron star. This “NS 1987A” is the youngest neutron star known near our galaxy, 51.4 kpc away in the Large Magellanic Cloud (Panagia 1999). After many years of unsuccessful searches for a pulsar or nonpulsing neutron star, which is difficult to find due to the dusty ejecta, indirect evidence has accumulated in recent years. Cigan et al. (2019) observed infrared emission from a relatively warm, compact blob of dust that Page et al. (2020) showed could be powered by a 30 yr old cooling neutron star. Greco et al. (2021, 2022) argue that the hard X-ray emission indicates the presence of a pulsar wind nebula.

Continuous gravitational-wave (GW) emission from NS 1987A has been suggested since Piran & Nakamura (1988). Such GWs could be produced by a nonaxisymmetric deformation of the neutron star, by free precession, or by long-lived r -mode oscillations, as summarized e.g., by Glampedakis & Gualtieri (2018).

The most recent search for continuous GW emission from NS 1987A used stochastic background methods to analyze data from Advanced LIGO and Virgo’s first three observing runs (Abbott et al. 2021a). Like previous similar searches referenced therein, Abbott et al. (2021a) assumed a small spin-down for NS 1987A. Of order 10^{-9} Hz s^{-1} , this spin-down is large by the standards of known pulsars but one or two orders of magnitude smaller than the spin-down implied by GW emission at a detectable level (see below).

Wette et al. (2008) scoped out broadband continuous GW searches for supernova remnants (such as 1987A) where there is evidence for a neutron star but pulses are not observed, and

hence a wide range of frequencies and spin-downs (time derivatives of the frequency) must be covered. (Continuous GW searches involve longer coherence times than stochastic background searches and typically search over spin-down parameters as well as GW frequencies.) The approach of Wette et al. (2008) was first used on the young neutron star in Cas A (Abadie et al. 2010), and similar methods have been used on other likely locations of neutron stars not observed as pulsars (Aasi et al. 2013a, 2015; Sun 2016; Zhu et al. 2016; Abbott et al. 2017, 2019; Dergachev et al. 2019; Ming et al. 2019; Lindblom & Owen 2020; Millhouse et al. 2020; Papa et al. 2020; Piccinni et al. 2020; Abbott et al. 2021b, 2022a; Jones & Sun 2021; Ming et al. 2022).

Wette et al. (2008) defined a key figure of merit, an indirect limit on GW emission similar to the spin-down limit for pulsars—i.e., a best-case amplitude of GW emission. Even when the spin-down is not known, one can assume that it has been dominated by GWs since the birth of the star and that it has spun the star down significantly from its birth frequency. This results in a frequency-independent limit based on the age of the star, extended by Owen (2010),

$$h_0^{\text{age}} = 2.5 \times 10^{-25} \left(\frac{51.4 \text{ kpc}}{D} \right) \left(\frac{30 \text{ yr}}{a} \right)^{1/2} \times \left(\frac{I}{10^{45} \text{ g cm}^2} \right)^{1/2} \left(\frac{6}{n-1} \right)^{1/2}. \quad (1)$$

Here h_0 is a measure of GW amplitude called the intrinsic strain (Jaranowski et al. 1998), D is the distance to the neutron star, a is its age, I is its moment of inertia, and $n = \ddot{f}/\dot{f}^2$ is its braking index. The braking index is about 5 or 7 if the GW emission is due to a corotating nonaxisymmetry (ellipticity) or an r -mode, respectively. The fiducial moment of inertia in Equation (1) is on the low end of the predicted range, and depending on the star’s mass and the nuclear matter equation of state, h_0 could go up by

Table 1
Parameters Used in Our Search

Input Parameters		Derived Parameters		
Name	Value	Name	Value (75–125 Hz)	Value (125–275 Hz)
Right ascension	05 ^h 35 ^m 28 ^s .0	Span	12.76 days	8.73 days
decl.	− 69°16′ 11″	Start	2017-06-22 20:29:29	2017-02-11 16:29:09
Age	30 yr	H1 SFTs	497	346
Distance	51.4 kpc	L1 SFTs	490	338

Note. The position was taken from the SIMBAD Database. Times are UTC.

about a factor of 2 (Abbott et al. 2021c), so the range of h_0^{age} for NS 1987A is about $2\text{--}4 \times 10^{-25}$.

Sun (2016) performed the most recent search for NS 1987A that used continuous GW methods, using the setup of Chung et al. (2011), and summarizing earlier searches for that star. Continuous wave methods are generally more sensitive than stochastic background methods but more computationally intensive. Because the Wette et al. (2008) wide parameter space was unfeasible for a source as young as NS 1987A (19 yr old for the data used and requiring a fourth spin-down parameter), Chung et al. (2011) narrowed the search by introducing a detailed spin-down model. But this is less robust than a model that makes few assumptions like Wette et al. (2008), and even with a narrow parameter space, Sun (2016) did not place upper limits beating the indirect limit h_0^{age} . Recent all-sky surveys for continuous GWs such as Abbott et al. (2022b) and Dergachev & Papa (2022) reach h_0^{age} in the direction of NS 1987A but cover too small a spin-down range for it.

As of Advanced LIGO and Virgo’s second observing run (O2) s, NS 1987A was 30 yr old. For that age and a 51.4 kpc distance (Panagia 1999), h_0^{age} is comparable to what recent GW searches of supernova remnants, such as Lindblom & Owen (2020), have achieved using only two spin-down parameters. The results of Wette et al. (2008) and Wette (2012) can be combined to estimate that a coherent search of O2 data can use only two spin-down parameters and surpass the sensitivity of h_0^{age} for a computing budget of order a million core-hours on a modern cluster.

Here we describe such a search, which detected no astrophysical signals but placed the first direct upper limits on the GW strain from NS 1987A to beat the indirect limit h_0^{age} over a wide and physically consistent parameter space.

2. Search Methods

Because our search methods were much like those of Lindblom & Owen (2020) and similar papers, we only summarize highlights and changes here and direct the reader to Lindblom & Owen (2020) and references therein for details. Our input parameters and some derived parameters are given in Table 1.

We used LIGO open data (Vallisneri et al. 2015; Abbott et al. 2021d) from O2, the most recent data publicly available when we started our computational runs, in the form of 1800 s short Fourier transforms (SFTs). O2 included data from the Hanford, WA (H1) and Livingston, LA (L1) 4 km interferometers. Once the integration time spans for our search bands were determined by computational cost (see below), we selected the stretch of data for each span to maximize

sensitivity, which is proportional to live time over the power spectral density (psd) of strain noise (Jaranowski et al. 1998).

The integration method was the multidetector \mathcal{F} -statistic (Jaranowski et al. 1998; Cutler & Schutz 2005), which efficiently accounts for the modulation of long-lived signals due to the rotation of Earth. Because $2\mathcal{F}$ is a quadrature of four matched filters, in stationary Gaussian noise it is drawn from a χ^2 distribution with four degrees of freedom.

We assumed that the demodulated signal frequency evolved in the solar system barycenter frame as

$$f(t) = f + \dot{f}(t - t_0) + \frac{1}{2}\ddot{f}(t - t_0)^2, \quad (2)$$

where the reference time t_0 is the beginning of the observation and the parameters (f, \dot{f}, \ddot{f}) are evaluated at that time. That is, we assumed no binary companion to NS 1987A, no glitches during the spans of integration, little timing noise, and insufficient frequency drift to require a third derivative.

To choose the parameter space—i.e., ranges of (f, \dot{f}, \ddot{f})—we first split the search into low- and high-frequency bands divided at 125 Hz, roughly twice the spin frequency of the fastest known young pulsar (Marshall et al. 1998). The latter should be the frequency of the most efficient emission of mass quadrupole GWs. For a given frequency f , the ranges of (\dot{f}, \ddot{f}) were chosen the same way as in Lindblom & Owen (2020). That is,

$$\begin{aligned} \frac{f}{(n_{\text{max}} - 1)a} &\leq -\dot{f} \leq \frac{f}{(n_{\text{min}} - 1)a}, \\ n_{\text{min}} \frac{\dot{f}^2}{f} &\leq \ddot{f} \leq n_{\text{max}} \frac{\dot{f}^2}{f}, \end{aligned} \quad (3)$$

with the braking index ranging from $n_{\text{min}} = 2$ to $n_{\text{max}} = 7$. These ranges correspond to a wide range of observed and predicted behaviors and are consistent with the minimum spin-down,

$$\begin{aligned} -\dot{f} &= 1.6 \times 10^{-8} \text{ Hz s}^{-1} \left(\frac{\mu}{2}\right)^2 \left(\frac{D}{51.4 \text{ kpc}}\right)^2 \\ &\times \left(\frac{h_0}{2 \times 10^{-25}}\right)^2 \left(\frac{f}{100 \text{ Hz}}\right) \left(\frac{10^{45} \text{ g cm}^2}{I}\right), \end{aligned} \quad (4)$$

required for a given h_0 —see, e.g., Owen (2010). Here, μ is the ratio of GW frequency to spin frequency. Note that the minimum value of $-\dot{f}$ is greater than the maximum value covered by all-sky surveys (Abbott et al. 2022b). The minimum frequency of the low band (75 Hz) and the maximum frequency of the high band (275 Hz) were chosen so that, according to the sensitivity estimate of Wette (2012), upper limits on h_0 would

just reach h_0^{age} . The precise value of h_0^{age} we chose for this purpose was the intermediate one displayed in Equation (1) for the r -mode emission from a low-mass (and moment of inertia) star or mass quadrupole emission from an intermediate-mass star, about 2.5×10^{-25} . For a computational cost of 10^6 core-hours per band, this resulted in the integration times and other parameters shown in Table 1.

The code was an improved version of that used in Lindblom & Owen (2020), based on the `S6SNRSearch` tag of the `LALSUITE` software package (LIGO Scientific Collaboration 2020) and its implementation of the \mathcal{F} -statistic. The search parameter space was split into roughly 10^5 batch jobs per band, each taking roughly 10 hr on the Texas Tech supercomputing cluster “Quanah.” We also used these jobs as an ad hoc way of clustering candidate signals. Event clusters included all candidates above the threshold from a job or nearby jobs. Each job covered all possible spin-down values for a distinct frequency band. Band widths ranged from 9.3×10^{-5} – 3.7×10^{-3} Hz, depending on frequency and integration time. At a template bank mismatch (Wette et al. 2008) of 0.2, parameter spacings in (f, \dot{f}, \ddot{f}) were roughly $(1.2 \times 10^{-6}$ Hz, 5×10^{-12} Hz s $^{-1}$, 3×10^{-18} Hz s $^{-2}$) and $(1.7 \times 10^{-6}$ Hz, 1.1×10^{-11} Hz s $^{-1}$, 9×10^{-18} Hz s $^{-2}$) for the low- and high-frequency bands, respectively. Total template counts were about 7×10^{13} and 9×10^{13} , respectively.

We did not a priori veto candidates based on time-frequency behavior or lists of known instrumental lines. Due to the rapid spin-down, a detectable signal would have, most templates overlap a spectral line for some time and such vetoes would render much of the search band unusable for setting upper limits. The rapid spin-down has the advantage, however, of diluting the effect of a narrow line on any given template, as the template relatively rapidly moves out of the disturbed frequency band. This is shown by the relatively small number of candidates (see below). We did use the interferometer consistency veto, a simple check first used in Aasi et al. (2013b) where the joint $2\mathcal{F}$ is greater than the value from either interferometer alone.

We performed consistency checks as in Lindblom & Owen (2020), plus two more necessitated by the unusual youth of the target and hence the high value of spin-downs searched: We confirmed that a third frequency derivative is not needed in Equation (2) and that the standard SFT length of 1800 s is not too long.

Inspection of the parameter space metric (Wette et al. 2008) shows that omitting the third frequency derivative can result in a substantial mismatch between signal and template for the parameters and integration times used here. However, Jaranowski & Krolak (2000) argued that correlations with lower derivatives allow for the third derivative to be ignored at much longer integration times than we use, while still keeping a low mismatch and thus a high fraction of the ideal $2\mathcal{F}$. Essentially, correlations allow a large template bank to pick up the signal efficiently at a shifted position (f, \dot{f}, \ddot{f}) . This argument is weak near the edges of parameter space, so we checked against a set of software injections (with the highest third derivatives allowed by our braking index range) and confirmed that omitting the third derivative causes no appreciable loss in $2\mathcal{F}$ for a population of signals. As Jaranowski & Krolak (2000) argue, there is no detectable effect.

One might expect the SFT length to be a problem for frequency derivatives high enough to send a signal through

multiple SFTs within the duration of one SFT, i.e., for $|\dot{f}|$ of order $1/(1800 \text{ s})^2$ or 3×10^{-7} Hz s $^{-1}$ —which is also the maximum $|\dot{f}|$ covered by our search. The injection checks of our upper limits (see below) already test this to some extent, but we performed additional injection studies dedicated to this issue. We found no significant losses for values up to 5×10^{-7} Hz s $^{-1}$, well beyond what we searched.

3. Search Results

We examined the search results for candidate signals surpassing 95% confidence in Gaussian noise, corresponding to $2\mathcal{F}$ thresholds of 77.1 and 77.5 for the low- and high-frequency bands respectively. (These values were determined using an effective number of independent templates found by a Kolmogorov–Smirnov distance minimizer between the observed distributions of the loudest events per search job and the Gaussian noise prediction. The effective number was almost the same as the number of templates.) The high band produced no candidates. The low band produced 29 search jobs with candidates mostly clustered around 83.32 and 100.0 Hz (4 jobs and 23 jobs in each cluster), with clusters limited to single jobs at 107.1 and 108.5 Hz. The highest $2\mathcal{F}$ was 95. We examined the search jobs as in Lindblom & Owen (2020) and found that all $2\mathcal{F}$ histograms and frequency plots showed contamination by broad noise lines. This was sufficient to rule out the candidates as astrophysical signals, but we followed up by checking against lists of known instrumental artifacts (Covas et al. 2018). The 83.32 and 100.0 Hz clusters are due to known lines in L1 and H1, respectively, and the one-job cluster at 108.5 Hz is due to a known line in H1. The one-job cluster at 107.1 Hz has $2\mathcal{F}$ improbably dominated by H1. The multijob clusters produced up to 0.1% of candidates triggering the interferometer consistency veto, several orders of magnitude above typical search jobs. Therefore, we do not claim any astrophysical signals in our search.

In the absence of signals, we set new astrophysically meaningful upper limits on intrinsic strain h_0 as a function of GW frequency in 1 Hz bands. The method was the same as in Lindblom & Owen (2020), with the same false dismissal rate of 10% (90% confidence) integrated over a population of sources with randomly oriented spin axes: A semianalytic estimate was confirmed with 1000 software-injected signals per upper limit band.

The left panel in Figure 1 displays our upper limits on h_0 as a function of frequency, minus two bands starting at 222 and 264 Hz, which the injections indicated had slightly more than a 10% false dismissal rate. The discontinuity at 125 Hz is due to the difference in integration times used above and below that frequency. The (red) horizontal line in the left panel represents the fiducial value of 2.5×10^{-25} of the indirect limit h_0^{age} from energy conservation. Our search places limits on GW emission from NS 1987A that are significantly better than this astrophysical upper limit over the band searched and better than the strictest h_0^{age} of 2.0×10^{-25} over part of the band.

The efficiency of our search can be expressed in terms of two quantities derived from h_0 . One common measure (Wette et al. 2008) is the factor Θ in

$$h_0 = \Theta \sqrt{S_h/T}, \quad (5)$$

where S_h is the harmonic mean psd of all SFTs and T is the total live time of data used. Our Θ is about 36 in the low-frequency band and 40 in the high-frequency band, slightly worse

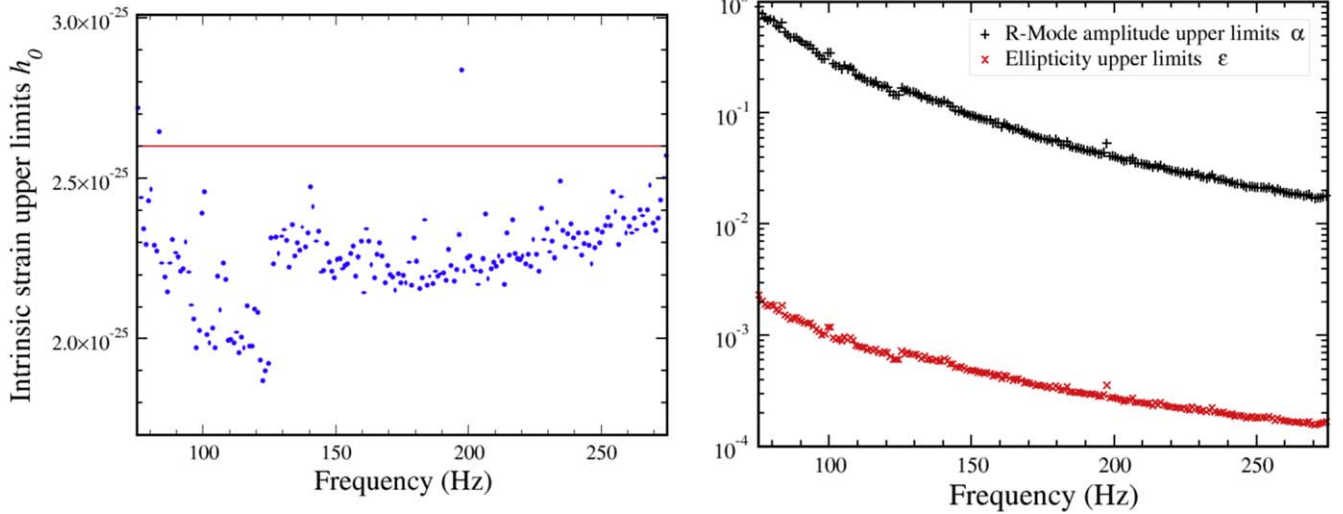


Figure 1. The left panel displays points representing direct observational 90% confidence upper limits on the intrinsic strain h_0 from NS 1987A as a function of frequency in 1 Hz bands for our search. The (red) horizontal line in the left panel indicates the indirect limit h_0^{age} from energy conservation. The right panel shows derived upper limits on the fiducial dimensionless neutron star ellipticity, ϵ , and r -mode amplitude, α , based on these h_0 upper limits. The h_0 data shown in the left panel is available in machine-readable format as the data behind the figure. (The data used to create this figure are available.)

(higher) than the youngest supernova remnant searches so far—see Lindblom & Owen (2020) for example. The sensitivity depth, defined by Behnke et al. (2015) as

$$D = \sqrt{S_h/h_0}, \quad (6)$$

is about $36 \text{ Hz}^{-1/2}$ and $29 \text{ Hz}^{-1/2}$ for the low and high bands, respectively. This is also slightly worse (lower) than the youngest supernova remnant searches so far, as expected due to the extreme youth and wide parameter space of NS 1987A.

Upper limits on h_0 can be converted to upper limits on fiducial neutron star ellipticity ϵ using (Wette et al. 2008, e.g.)

$$\epsilon \simeq 9.5 \times 10^{-5} \left(\frac{h_0}{1.2 \times 10^{-24}} \right) \left(\frac{D}{1 \text{ kpc}} \right) \left(\frac{100 \text{ Hz}}{f} \right)^2, \quad (7)$$

and to upper limits on a particular measure of r -mode amplitude, α (Lindblom et al. 1998), using Owen (2010),

$$\alpha \simeq 0.028 \left(\frac{h_0}{10^{-24}} \right) \left(\frac{100 \text{ Hz}}{f} \right)^3 \left(\frac{D}{1 \text{ kpc}} \right). \quad (8)$$

The numerical values are uncertain by a factor of roughly 2 or 3 due to uncertainties in the unknown neutron star mass and equation of state. Upper limits on ϵ and α for NS 1987A from this search are shown in the right panel of Figure 1. Indirect limits on ϵ and α derived from h_0^{age} are not shown because, on this logarithmic scale, they are close to the direct observational limits.

Our upper limits on h_0 beat the indirect limit h_0^{age} . The latter limit is astrophysically interesting despite the youth of the source. Equation (1) is derived under the assumption that the star has spun down significantly since birth. Without that assumption, but with constant braking index n , the limit h_0^{age} is multiplied by Sun (2016),

$$[1 - (f_b/f)^{1-n}]^{1/2}, \quad (9)$$

where f_b is the GW frequency at birth. If $f \ll f_b$, this factor is 1, and we recover Equation (1). If $f_b \approx f$ as assumed by Sun (2016), essentially imposing a smaller ellipticity, this factor can be much less than 1, but it does not need to be. It is straightforward to use our direct limits on ϵ and α to integrate \dot{f} and find that after 30 yr f is low enough that the factor in Equation (9) is about 1. This means that Equation (1) holds even for NS 1987A. Thus, our search had a chance of detecting a signal, and the lack of detection represents the first GW observational constraints on NS 1987A.

4. Conclusions

We have performed the first search for GWs from NS 1987A that covered a physically consistent range of spin-downs and achieved a sensitivity better than the indirect limit from energy conservation. We also showed that this limit is applicable to NS 1987A despite the youth of the source. While we detected no astrophysical signal, we set direct observational upper limits that beat the indirect limit and thus for the first time constrain the GW emission of NS 1987A if it is emitting within the frequency band searched. Our constraints on the r -mode amplitude are not competitive with the standard theoretical prediction (Bondarescu et al. 2009), but our constraints on ellipticity are within the predicted range of elastic deformations of quark stars (Owen 2005). If NS 1987A is made of baryonic matter and the protons in its core are not yet superconducting, our constraints imply upper limits on the internal magnetic field of about 10^{15} G for the twisted torus configuration likely formed with the neutron star (Ciolfi & Rezzolla 2013). If the protons are now superconducting, the field is likely mainly poloidal and our constraints limit the field to less than about 10^{16} G (Lander 2014).

Our search achieved this with a simple coherent integration of O2 data. Better methods and data are available, and we expect this will motivate further searches and improvements of search methods for rapidly evolving continuous wave signals.

This research has made use of data, software, and/or web tools obtained from the Gravitational Wave Open Science Center (<https://www.gw-openscience.org>), a service of LIGO Laboratory, the LIGO Scientific Collaboration, and the Virgo Collaboration. LIGO is funded by the U.S. National Science Foundation. Virgo is funded by the French Centre National de Recherche Scientifique (CNRS), the Italian Istituto Nazionale della Fisica Nucleare (INFN), and the Dutch Nikhef, with contributions by Polish and Hungarian institutes. This research was supported in part by NSF grants PHY-2012857 to the University of California at San Diego and PHY-1912625 to Texas Tech University. This work was completed in part at the Aspen Center for Physics, which is supported by National Science Foundation grant PHY-1607611. The authors acknowledge computational resources provided by the High Performance Computing Center (HPCC) of Texas Tech University at Lubbock (<http://www.depts.ttu.edu/hpcc/>). We are grateful to Katharine Long and Joseph Romano for comments on the manuscript.

ORCID iDs

Benjamin J. Owen  <https://orcid.org/0000-0003-3919-0780>

References

- Aasi, J., Abadie, J., Abbott, B. P., et al. 2013a, *PhRvD*, **88**, 102002
Aasi, J., Abadie, J., Abbott, B. P., et al. 2013b, *PhRvD*, **87**, 042001
Aasi, J., Abbott, B. P., Abbott, R., et al. 2015, *ApJ*, **813**, 39
Abadie, J., Abbott, B. P., Abbott, R., et al. 2010, *ApJ*, **722**, 1504
Abbott, B. P., Abbott, R., Abbott, T. D., et al. 2019, *ApJ*, **875**, 122
Abbott, R., Abbott, T. D., Abraham, S., et al. 2021a, *PhRvD*, **104**, 022005
Abbott, R., Abbott, T. D., Abraham, S., et al. 2021b, *ApJ*, **921**, 80
Abbott, R., Abbott, T. D., Abraham, S., et al. 2021c, *ApJ*, **922**, 71
Abbott, R., Abbott, T. D., Abraham, S., et al. 2021d, *SoftX*, **13**, 100658
Abbott, R., Abbott, T. D., Acernese, F., et al. 2022a, *PhRvD*, **105**, 082005
Abbott, R., Abe, H., Acernese, F., et al. 2022b, arXiv:2201.00697
Abbott, B. P., Abbott, R., Abbott, T. D., et al. 2017, *PhRvD*, **95**, 082005
Behnke, B., Papa, M. A., & Prix, R. 2015, *PhRvD*, **91**, 064007
Bionta, R. M., Blewitt, G., Bratton, C. B., et al. 1987, *PhRvL*, **58**, 1494
Bondaescu, R., Teukolsky, S. A., & Wasserman, I. 2009, *PhRvD*, **79**, 104003
Chung, C., Melatos, A., Krishnan, B., & Whelan, J. T. 2011, *MNRAS*, **414**, 2650
Cigan, P., Matsuura, M., Gomez, H. L., et al. 2019, *ApJ*, **886**, 51
Ciolfi, R., & Rezzolla, L. 2013, *MNRAS*, **435**, L43
Covas, P. B., Effler, A., Goetz, E., et al. 2018, *PhRvD*, **97**, 082002
Cutler, C., & Schutz, B. F. 2005, *PhRv*, **D72**, 063006
Dergachev, V., & Papa, M. A. 2022, arXiv:2202.10598
Dergachev, V., Papa, M. A., Steltner, B., & Eggenstein, H.-B. 2019, *PhRvD*, **99**, 084048
Glampedakis, K., & Gualtieri, L. 2018, *The Physics and Astrophysics of Neutron Stars*, Astrophysics and Space Science Library, Vol. 457 (Cham: Springer), 673
Greco, E., Miceli, M., Orlando, S., et al. 2021, *ApJL*, **908**, L45
Greco, E., Miceli, M., Orlando, S., et al. 2022, *ApJ*, **931**, 132
Hirata, K., Kajita, T., Koshihara, M., et al. 1987, *PhRvL*, **58**, 1490
Jaranowski, P., & Krolak, A. 2000, *PhRvD*, **61**, 062001
Jaranowski, P., Krolak, A., & Schutz, B. F. 1998, *PhRv*, **D58**, 063001
Jones, D., & Sun, L. 2021, *PhRvD*, **103**, 023200
Lander, S. K. 2014, *MNRAS*, **437**, 424
LIGO Scientific Collaboration 2020, LIGO Algorithm Library—LALSuite, free software (GPL), doi: [10.7935/GTIW-FZ16](https://doi.org/10.7935/GTIW-FZ16)
Lindblom, L., & Owen, B. J. 2020, *PhRvD*, **101**, 083023
Lindblom, L., Owen, B. J., & Morsink, S. M. 1998, *PhRvL*, **80**, 4843
Marshall, F. E., Gotthelf, E. V., Zhang, W., Middleditch, J., & Wang, Q. D. 1998, *ApJL*, **499**, L179
Millhouse, M., Strang, L., & Melatos, A. 2020, *PhRvD*, **102**, 083025
Ming, J., Papa, M. A., Eggenstein, H.-B., et al. 2022, *ApJ*, **925**, 8
Ming, J., Papa, M. A., Singh, A., et al. 2019, *PhRvD*, **100**, 024063
Owen, B. J. 2005, *PhRvL*, **95**, 211101
Owen, B. J. 2010, *PhRv*, **D82**, 104002
Page, D., Beznogov, M. V., Garibay, I., et al. 2020, *ApJ*, **898**, 125
Panagia, N. 1999, *IAUS*, **190**, 549
Papa, M. A., Ming, J., Gotthelf, E. V., et al. 2020, *ApJ*, **897**, 22
Piccinni, O. J., Astone, P., D'Antonio, S., et al. 2020, *PhRvD*, **101**, 082004
Piran, T., & Nakamura, T. 1988, *PTEP*, **80**, 18
Sun, L., Melatos, A., Lasky, P. D., Chung, C. T. Y., & Darman, N. S. 2016, *PhRvD*, **94**, 082004
Vallisneri, M., Kanner, J., Williams, R., Weinstein, A., & Stephens, B. 2015, *J. Phys. Conf. Ser.*, **610**, 012021
Wette, K. 2012, *PhRvD*, **85**, 042003
Wette, K., Owen, B. J., Allen, B., et al. 2008, *CQGra*, **25**, 235011
Zhu, S. J., Papa, M. A., Eggenstein, H.-B., et al. 2016, *PhRvD*, **94**, 082008